

Comparison of thermodynamic stabilities and mechanical properties of CO₂, SiO₂, and GeO₂ polymorphs by first-principles calculations

Mia Ledyastuti, Yunfeng Liang, Caetano R. Miranda, and Toshifumi Matsuoka

Citation: *The Journal of Chemical Physics* **137**, 034703 (2012); doi: 10.1063/1.4735077

View online: <http://dx.doi.org/10.1063/1.4735077>

View Table of Contents: <http://scitation.aip.org/content/aip/journal/jcp/137/3?ver=pdfcov>

Published by the [AIP Publishing](#)

Articles you may be interested in

First-principles study of Ge dangling bonds with different oxygen backbonds at Ge/GeO₂ interface
J. Appl. Phys. **111**, 076105 (2012); 10.1063/1.3702816

First-principles study of Ge dangling bonds in GeO₂ and correlation with electron spin resonance at Ge/GeO₂ interfaces
Appl. Phys. Lett. **99**, 212103 (2011); 10.1063/1.3662860

Electronic, optical and thermal properties of the hexagonal and rocksalt-like Ge₂Sb₂Te₅ chalcogenide from first-principle calculations
J. Appl. Phys. **110**, 063716 (2011); 10.1063/1.3639279

Thermodynamic stability boundaries of “classical” noble-gas crystals and the polymorphism problem
Low Temp. Phys. **37**, 595 (2011); 10.1063/1.3645008

Structural stability of polymeric nitrogen: A first-principles investigation
J. Chem. Phys. **132**, 024502 (2010); 10.1063/1.3290954



Re-register for Table of Content Alerts

Create a profile.



Sign up today!



Comparison of thermodynamic stabilities and mechanical properties of CO₂, SiO₂, and GeO₂ polymorphs by first-principles calculations

Mia Ledyastuti,¹ Yunfeng Liang,^{1,a)} Caetano R. Miranda,^{1,2,a)} and Toshifumi Matsuoka^{1,a)}

¹Environment and Resource System Engineering, Kyoto University, Kyoto 615-8540, Japan

²Universidade Federal do ABC, Rua Santa Adélia, 166 Bangu 09210-170, Santo André, SP Brazil

(Received 27 April 2012; accepted 21 June 2012; published online 18 July 2012)

The recent discovery that molecular CO₂ transforms under compression into carbon four-coordinated, 3-dimensional network solid phases has generated considerable interests on possible new phases in the fourth-main-group elemental oxides. Based on density-functional theory calculations, we have investigated the thermodynamic stability, mechanical properties and electronic structure of proposed guest-free clathrates, quartz and cristobalite phases for CO₂, SiO₂, and GeO₂, and the dry ice phase for CO₂. It was predicted that a GeO₂ clathrate, likely a semiconductor, could be synthesized presumably with some suitable guest molecules. The hypothetical CO₂ guest-free clathrate phase was found hardly to be formed due to the large energy difference with respect to the other polymorphs. This phase is unstable at all pressures, which is also implied by its different electronic structure in comparison with SiO₂ and GeO₂. Finally, the SiO₂ clathrate presents a uniquely high bulk modulus, which is higher than that of quartz and three times of the experimental data, might not be a weak point of *ab-initio* calculations such as pseudopotentials, correlation functional etc., instead it can be readily understood by the constraint as imposed by the high symmetry. Either temperature or an “exhausted” relaxation (without any symmetry constraint) can remedy this problem. © 2012 American Institute of Physics. [<http://dx.doi.org/10.1063/1.4735077>]

I. INTRODUCTION

The diversity of SiO₂ phase diagram is known for a long term; however, the elemental oxide counterparts as CO₂ and GeO₂ present much more limited crystalline phase variability. The relative small free energy difference between SiO₂ phases as a function of temperature and pressure provides the formation of several four-coordinated 3-dimensional network solid phases such as quartz, cristobalite, tridymite, keatite, and their respective high symmetry phases.

Recently, it was reported that CO₂ can also form a non-molecular solid phase, known as CO₂ phase V, by compressing CO₂ phase III at pressures above 40 GPa and 1800 K.¹ Upon this new finding, the x-ray diffraction pattern has revealed that the structure of this “superhard” 3-dimensional network solid CO₂ is similar to P2₁2₁2₁ SiO₂ tridymite.² However, the intensity data and the preferred orientation in their study² didn't allow a rigorous structural refinement. On the other hand, theoretical work has suggested the β -cristobalite-like ($I\bar{4}2d$) as a stable phase for 3-dimensional network solid CO₂ at high pressure.³ This phase has also been verified unequivocally by using synchrotron x-ray diffraction and optical spectroscopies such as Raman and infrared spectra, very recently.⁴⁻⁶ Extended compression of CO₂ phase III at room temperature between 40-80 GPa gives a four-fold coordinated silica-like amorphous structure called carbonia.⁷ In case of GeO₂, Smith and Isaacs have determined a quartz-like GeO₂ structure by x-ray diffraction.⁸ The six coordination

paradigm in GeO₂ has changed to include the four coordination, as observed in SiO₂, while the stable phase at ambient temperature and pressure is the six-coordinated rutile. These silica-like phases suggest the possibility of the appearance of other crystalline phases for fourth-main-group elemental oxides in parallel to the observed SiO₂ polymorphs.

A very interesting SiO₂ four-fold coordinated phase is the clathrate structure family compounds (Figure 1), which were originally proposed for hydrates systems. The cage structure in clathrates allows the trapping from simple molecules like CO₂ and CH₄ or mixture of them to complex ones.⁹⁻¹⁵ A similar crystalline structure for SiO₂ clathrate called melanophlogite exist in nature as a rare mineral.¹⁶⁻²⁰ This mineral has cubic structure with space group $Pm\bar{3}n$, which is the structural analog of type I crystalline hydrate.¹⁷ It shows slightly distorted structure with a lower symmetry when the temperature is decreased.^{18,21} The existence of melanophlogite encourages the possibility to have similar clathrate structures of CO₂ and GeO₂.

The knowledge of the stability diagram of energy as function of volume or pressure can be a tool to verify the thermodynamics and mechanical properties of materials. It can provide an important step to guide for possible routes of new materials synthesis. Nowadays, computational materials science methods can help to determine the thermodynamics of materials with high accuracy and propose new routes for their synthesis before the usually expensive and time-consuming trial and error experiments.²²

In this report, we provide a comparison between existing crystalline phases of CO₂, SiO₂ and GeO₂ to proposed clathrate based structures. To construct the phase stability

^{a)}Authors to whom correspondence should be addressed. Electronic addresses: caetano.miranda@ufabc.edu.br, y_liang@earth.kumst.kyoto-u.ac.jp, and matsuoka@earth.kumst.kyoto-u.ac.jp.

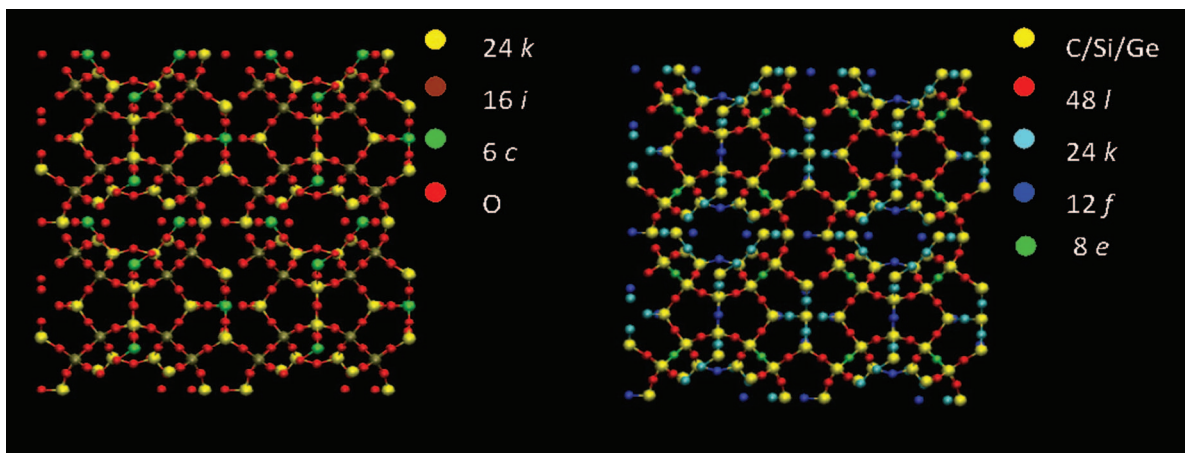


FIG. 1. Crystal structure of CO₂, SiO₂ and GeO₂ clathrate. Carbon, silicon, and germanium were classified into three sites (24*k*, 16*i* and 6*c*); meanwhile, oxygen was classified into four sites (48*l*, 24*k*, 12*f*, and 8*e*).

diagrams, we have chosen several stable polymorphs for CO₂, SiO₂ and GeO₂ as reference for our proposed guest-free clathrate type I systems. Dry ice, known as CO₂-I, is face centered cubic structure with *Pa3* symmetry space group and stable at low temperature and pressure^{23–25} has been chosen as reference of CO₂ phases. The α -quartz phase, which is observed in both SiO₂ and GeO₂, can be a good reference at higher pressure.^{26,27} The β -cristobalite phase, which is found as a SiO₂ polymorph and also recently proposed for CO₂ systems, was also chosen as reference.^{28–30} Slightly different phases should be used for GeO₂ case, where we have included rutile, which is six-coordinated phase as reference due to the stability at ambient condition.^{31,32} Here, we have studied the stability, mechanical and electronic properties of proposed guest-free clathrates of CO₂, SiO₂, and GeO₂ in comparison with their respective stable phases by first principles calculations.

II. METHODOLOGY

The total energy of the elemental oxide phases were determined by first principles calculation within the Density Functional Theory as implemented in the VASP package.³³ The generalized gradient approximation (GGA)^{34,35} and meta-GGA³⁶ were implemented for all the systems. In GGA, the exchange correlation energy is dependent on local gradient of the electron density, meanwhile the meta-GGA introduces kinetic energy density as an additional feature.³⁶ The GGA corrects the overestimation of bond strength in oxides, which gives smaller lattice constant values, but it was reported to fail in describing the stability of silica polymorphs. In GGA, cristobalite is more stable at 0 GPa and 0 K than quartz, which is in contrast with experimental observations.³⁷ To solve this problem for SiO₂ polymorphs, we have also used the meta-GGA, which likely represents more accurate in energy prediction.³⁶ The project augmented wave (PAW) pseudopotential was used to treat core and valence electrons with s2p2 valence configuration for C, Si and Ge, and s2p4 for O atoms. For all systems, all atoms were allowed to relax using conjugated gradient methods until the forces are smaller than 0.04 eV/Å, while the cell shape was kept fixed. Through this

scheme, the accuracy of the energy values is at the order of 0.1 meV or less. The total energy for all systems was converged with respect to the Brillouin-zone sampling integration and energy cut-off of 550 eV was used. Bulk modulus was determined by fitting the energy curve as function of volume with respect to the Birch-Murnaghan equation of state.

We also combined first-principles calculation with classical molecular dynamics to explain the anomalies of material, which is found in SiO₂ guest-free clathrate. The parameterized potential, to fit first principles forces, energies and pressures, developed by Tangney and Scandolo, was chosen as SiO₂ force field.³⁸ This potential has shown to capture the correct phases for SiO₂ and reproduce most of the observed anomalies of the silica.^{21,38–42} The simulation started from 46 SiO₂ molecules clathrate framework with a time step ~ 0.72 fs (30 a.u.) in NPT ensemble at range -10 to 10 GPa of pressure. The trajectory was performed up to 21.6 ps at selected temperature 0 and 300 K then the configuration was analyzed.

III. RESULTS AND DISCUSSIONS

A. Phase stability

The calculated equation of states for CO₂ polymorphs is shown in Fig. 2. Dry ice has proved to be the most stable CO₂ polymorph at 0 GPa at least within the phases considered here, followed by β -cristobalite with *I42d* space group, α -quartz and the guest-free CO₂ clathrate. Our work indicates a good agreement with previous calculations for the relative stabilities between CO₂ polymorphs. Previously, α -quartz-like structure was found to be stable phase at high pressure²⁶ but then the discovery of β -cristobalite-like structure with *I42d* space group shows even lower energy.²⁷ In fact, *I42d* β -cristobalite has become reference to determine the stability of CO₂ solid higher coordination number such as α -PbO₂, CaCl₂, stishovite and pyrite.^{28–30} Similar to previous studies, we also found β -cristobalite as the most stable phase at high pressure, as it can be seen in Fig. 3. Our proposed guest-free clathrate shows higher enthalpy compared with other CO₂ phases. In our calculations, we notice that for negative pressures below (~ -11 GPa) the guest-free clathrate

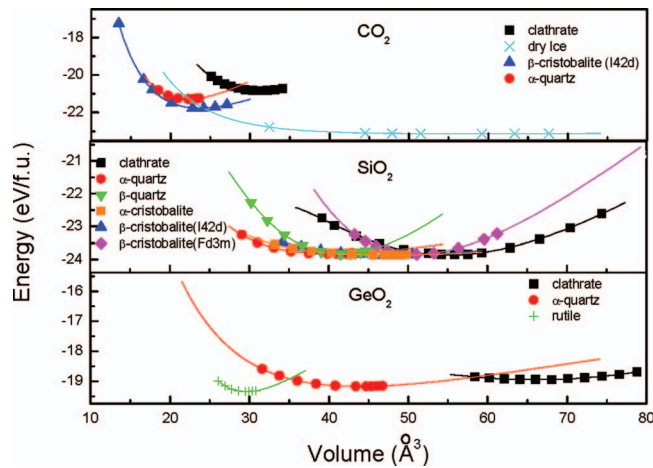


FIG. 2. The energy as function of CO_2 , SiO_2 and GeO_2 volume. The “f.u.” in the y-axis stands for formula unit. I42d stands for $I\bar{4}2d$. Fd3m stands for $Fd\bar{3}m$.

transforms to molecular phase during the relaxation process and for pressures above (~ 70 GPa), the system was found to be structurally and topologically amorphized. The CO_2 guest-free clathrate has energy difference with respect to the nearest phase α -quartz-type structure of 1.2 eV per CO_2 unit at 0 GPa. This difference increases with increasing pressure. This indicates that the possibility to synthesize the CO_2 guest-free clathrate is thermodynamically difficult.

As expected, for the SiO_2 guest-free clathrate, we noticed its stability from the equation of states in Fig. 2. The difference among different phases is in average around 0.02 eV per SiO_2 unit. The binding energy of natural SiO_2 guest-free clathrate, i.e., melanophlogite, is unknown. But from experiment, the cubic structure guest-free melanophlogite has $52.12 \text{ \AA}^3/\text{SiO}_2$ of volume,¹⁹ slightly smaller than our guest-free clathrate ($55.08 \text{ \AA}^3/\text{SiO}_2$). In SiO_2 case, all polymorphs have shown a similar minimal relaxed energy. Based on this fact, we can understand the extraordinary richness of SiO_2 low-pressure polymorphs. The α -quartz is most stable phase

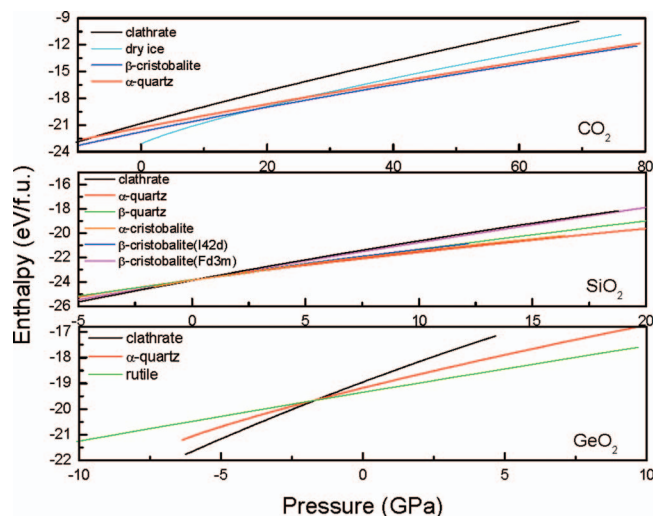


FIG. 3. The enthalpy of CO_2 , SiO_2 and GeO_2 polymorphs as function of pressure.

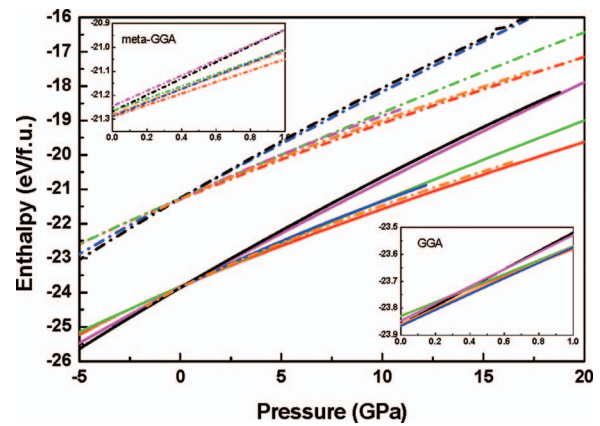


FIG. 4. Comparison of GGA and meta-GGA calculation of several SiO_2 polymorphs. Inset: the enthalpy as function of pressure from GGA and meta-GGA was shown within a range of 1.0 GPa.

for SiO_2 at ambient condition, but from our calculation β -cristobalite has the lowest energy. Our result is similar to the previous results, where GGA was also implemented in their calculation for several SiO_2 polymorphs.³⁷ In this particular case, it has proved to be a limitation of GGA in the total energy calculation. With the use of Meta-GGA based functional, our calculations show a stability phase sequence of SiO_2 polymorphs in agreement with experimental observations for the phases studied. In Fig. 4, the energy of the β -cristobalite ($I\bar{4}2d$ and $Fd\bar{3}m$ space group) at 0 GPa is higher than α -quartz, which shows good agreement with experimental results. The crystal structures of β -cristobalite had been under debate and three kinds of space groups, $P2_13$, $I\bar{4}2d$ and the “ideal” $Fd\bar{3}m$ have been proposed over many years.⁴³ It is now being clear that the β -cristobalite has a cubic $Fd\bar{3}m$ structure in average, however, with the oxygen dynamically rotating along the Si-Si axis^{42–44}. In this work, only two kinds of β -cristobalite, $I\bar{4}2d$ and ideal $Fd\bar{3}m$, have been considered in order to demonstrate the consequence of the different symmetry upon the mechanical properties (as discussed in Sec. III B).

For GeO_2 , the most stable phase occurred, when the germanium atom surrounded by six oxygen atoms. Our calculation has shown rutile, which has trigonal symmetry as the phase with lowest energy at 0 GPa as shown in Fig. 2. This is corresponding to the experimental results, where the most stable phase of GeO_2 at ambient condition is rutile. This phase has structure similar to stishovite in SiO_2 and transforms into α -quartz-like structure at high temperature and ambient pressure. The stability of high coordination number phase GeO_2 might be a consequence of the more metallic character of germanium compared with carbon and silicon³⁰ and geometry constraint of cation/anion radius ratio, for which germanium is at the size limit for 4-fold coordination.⁴⁵ Quartz phase becomes the second stable phase then followed by guest-free clathrate. In the variation of pressure, GeO_2 has similarities with SiO_2 where both change their coordination number from four to six at high pressure and may serve as archetypal materials of minerals, however the phase transition occurs at much lower pressure.³² Although less stable than the other phases, the guest-free clathrate may still be possible to be synthesized.

The energy difference between guest-free clathrate with α -quartz, which is the nearest phase, is only around 0.2 eV per GeO_2 unit. This condition may allow the synthesis of GeO_2 guest-free clathrate. In addition, it becomes the most stable phase at pressures lower than -2 GPa (Fig. 3). Finally, it is interesting to note that the enthalpy of the rutile-type, quartz-type and clathrate-type GeO_2 have a common crossing point, namely, the transition of rutile-type GeO_2 into clathrate-type GeO_2 would be at a thermodynamic condition (presumably with a suitable guest molecules) close to the formation condition of quartz-like structure.

B. Mechanical properties

Beside the thermodynamic stability, we also calculated the mechanical strength for CO_2 , SiO_2 and GeO_2 polymorphs. The detailed mechanical properties CO_2 , SiO_2 and GeO_2 polymorphs are summarized in Table I. Dry ice phase with its energy profile almost flat in variation of volume has the lowest mechanical strength shown by very-small bulk modulus value. This is already anticipated, as dry ice is a molecular solid that intermolecular interaction is very weak.^{24–26} In non-molecular solid of CO_2 , α -quartz has higher bulk modulus than β -cristobalite, as reported by previous work.²⁷ Among all the tetrahedral phases that we have considered for SiO_2 , α -cristobalite and β -quartz presents the lowest and the highest bulk modulus, respectively. Our result has a good agreement with the previous work.³⁷ The bulk modulus of GeO_2 polymorph also has a good agreement with previous calculations.³¹ In general, CO_2 at the analogous phase has higher bulk modulus than SiO_2 and GeO_2 . For example, CO_2 quartz phase has 182.2 GPa of bulk modulus, different by almost one order of magnitude than SiO_2 (32.7 GPa). The hardness of CO_2 solid is caused by the stronger chemical bond between carbon and oxygen, as reflected by the short C-O bond length and the rigidity of inter tetrahedral bridging angle C-O-C.²⁷ In case of the clathrates, the calculated C-O bond length is 1.40 Å is much shorter than the Si-O bond length (~ 1.61 Å) and Ge-O bond length (~ 1.77 Å). The C-O-C band

angle (143.7°) is smaller than Si-O-Si bond angle (168.2°) and comparable to the Ge-O-Ge angle (147.2°). The inter-tetrahedral angle profile of CO_2 can be the answer of the limitation of CO_2 3-dimensional network solid phases. It has been shown previously that the angle profile of CO_2 β -cristobalite is very steep like “bull’s eye” pattern, meanwhile for SiO_2 ’s pattern is “thumb print”.³ The electronic properties of CO_2 and SiO_2 also support the small C-O-C angle values. As discussed in Sec. III C, the value of electronic charge around carbon atom is lower than the corresponding silicon atom thus makes the C-O bond more covalent than Si-O bond.

For SiO_2 clathrate phase, we found bulk modulus of SiO_2 guest-free clathrate (70.1 GPa) is higher than that of quartz and the experimental data, which is rather surprising. Based on the x-ray diffraction analysis, the bulk modulus of guest-free melanophlogite is 23–26.3 GPa,^{19,20} which are much lower than our calculation and is almost 1/3 of our calculated value. We assume that different bulk modulus values might be due to the temperature effect in experiment (300 K) compared with our first principles calculation (0 K). Thus, we calculated the SiO_2 guest-free clathrate by classical molecular dynamics at 0 and 300 K, respectively. The bulk modulus decreases with increasing temperature. For 300 K, the bulk modulus is found to be 30.8 GPa, in close agreement with the experimental values. Interestingly, if we perform an “exhausted” long relaxation, a second minimum (State II in Fig. 5) was presented as shown in Fig. 5. The second minimum was not detected by first principles calculation, because in this calculation the symmetry of structure was kept fixed. In the classical molecular dynamics (steepest descent), this constraint was not applied. Thus, the configuration in the second minimum was expected to have a different symmetry with respect to the first minimum (State I in Fig. 5). Our analysis showed a low symmetry $\text{p}\bar{1}$ (State II in Fig. 5) in the last configuration and the bulk modulus was rather close to the experiment 35.6 GPa. We suggest the decrease and wider distribution of Si-O-Si angle (as shown in Figs. 5(b) and 5(d)) is responsible for this bulk modulus deviation. We found that the average Si-O-Si angle decreases significantly with the increasing of temperature, from 164.5° at 0 K to 151.0° at 300 K, respectively. As shown in Fig. 5(c), the Si-O-Si angle has been re-distributed and widened. The softening of material along temperature increase is common for most minerals, the intermolecular rotation much easier at higher temperature. The same fact was also found in longer relaxation simulation, intermolecular Si-O-Si angle drop to 149.1° from 164.5° . The loss of symmetry might also be a sign of the instability of the high symmetry SiO_2 guest-free clathrate structure, which is in good agreement with the experimental findings, where a slightly distorted structure with a lower symmetry was formed with decreasing temperature.^{17,20} It is noteworthy to remark that the high-symmetry phase may be stable at high temperature with a dynamically disordered structure (extremely anharmonic),^{42–44} however, the structure in average can be of very high symmetry. This is indeed the case, for β -quartz and the β -cristobalite of SiO_2 with an $Fd\bar{3}m$ symmetry, where an exotic bulk modulus was obtained at 0K (Table I). We strengthen that the latter is not a weak point of *ab initio* calculations such as pseudopotentials, correlation functional etc.,

TABLE I. The bulk modulus of some CO_2 , SiO_2 and GeO_2 solid phase derived from fit energy curve to Birch-Murnaghan equation of states.

Phase	Bulk Modulus (GPa)		
	CO_2	SiO_2	GeO_2
Dry Ice	2.09 (3.21) ^a
α -quartz	182.2 (205.7) ^b	32.7 (31.3) ^c	33.0 (37.7) ^d
β -quartz	...	130.9 (121.6) ^c	...
α -cristobalite	(142.8) ^b	12.3 (9.4) ^c	...
β -cristobalite ($I\bar{4}2d$)	131.4 (149.1 ^b , 136 ^e)	21.6 (21.7) ^c	...
β -cristobalite ($Fd\bar{3}m$)	...	129.4 (119.5) ^c	...
Rutile	(310) ^f	(261) ^c	205.6 (267) ^d
Guest-free Clathrate	141.5	75.1	35.2

^aReference 26.

^bReference 27.

^cReference 37.

^dReference 31.

^eReference 5.

^fReference 28.

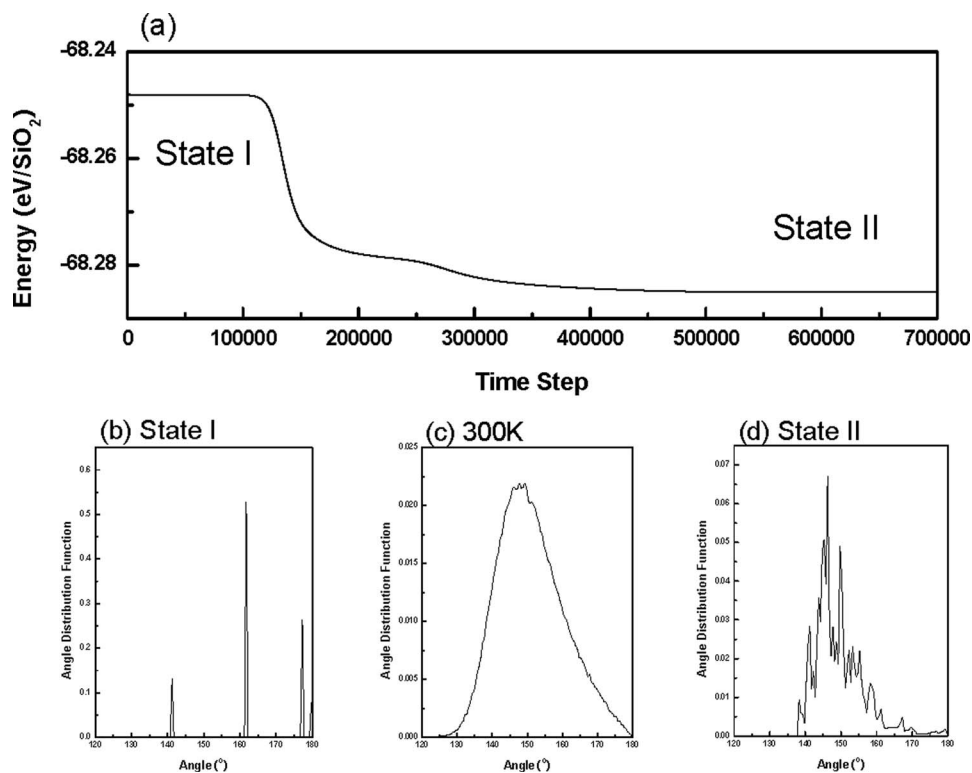


FIG. 5. The “temporal” evolution of enthalpy for classical molecular dynamics (steepest descent) of SiO_2 guest-free clathrate at 0 GPa and 0 K (a). Structure at the initial stage has cubic symmetry $Pm\bar{3}n$ space group (State I). Low symmetry structure with a $p\bar{1}$ space group was State II. The angle distribution function of Si-O-Si of these two configurations (States I and II) were shown in (b) and (d) in comparison with the angle distribution of Si-O-Si at 300 K (c).

instead it can be readily understood by the constraint as imposed by the high symmetry as shown here for SO_2 clathrate. To this end, cautions must be taken when a high-temperature phase was investigated at 0 K. Finally, it is perhaps very appropriate to mention it here that the phase V of CO_2 is a truly ordered tetragonal structure with space group of $I\bar{4}2d$, which, in this aspect, differs from the β -cristobalite of SiO_2 .⁴⁻⁶

C. Electronic structure

To better understand the differences of the elemental oxide polymorph within the same structure, we have also investigated the electronic properties of the clathrate systems under this perspective. The charges were determined by using Bader analysis.⁴⁶ Additionally, the electron localization function (ELF) was used to probe the bonding nature between atoms.⁴⁶⁻⁴⁹ Qualitatively, the ELF can be used as tool for locating nonbonding electron pairs and the bonding electrons.^{33,36} This function is defined between 0 and 1, where a value close to 1 means strong localization characteristics of covalent bonds or lone electron pairs. Values close to 0.5 reflect an electron-gas type.

The carbon atom in the CO_2 clathrate structure has Bader charge values around 1.94 and 7.03 (−1.03 net charge) for oxygen atom, which indicates a covalent bonding type. The obtained electron localization function is shown in Fig. 6. The “free electron gas” (with isosurface values close to 0.5, here, 0.506) can be seen only surrounding oxygen atom (Fig. 6(a)). This indicates a dominant polarization of oxygen in the oxide. The strongly localized electrons with isosurface values

close to 1 (here, 0.894) are observed in the outer shell of oxygen atom with a “banana” shape, namely, they are the non-bonding lone electron pairs (Fig. 6(b)).

The electronic structure of SiO_2 clathrate is slightly different from the CO_2 clathrate. The Bader analysis showed bonding in this molecule more ionic than CO_2 clathrate. The Bader silicon charge was calculated around 0.81 meanwhile oxygen atom charge is around 7.59 (−1.59 net charge), which suggests a partially electron transfer from silicon atom to oxygen ones, indicating an ionic-like character. The free electron gas is surrounding oxygen atom as shown in Fig. 5(c), while strongly localized electrons are observed in the outer shell of oxygen atom and at the oxygen-silicon atom boundary as shown in Fig. 6(d). The shape of free electron gas of SiO_2 clathrate is the same as the one found for CO_2 clathrate, as well as their non-bonding electrons presenting a similar banana shape. The difference is for the strongly localized electrons, which is located at the oxygen-silicon atom boundary and being of bonding state.

The GeO_2 clathrate shows Bader charges closer to the CO_2 than SiO_2 clathrate. The charge of germanium was found to be 1.72, while the oxygen is around 7.14 (−1.14 net charge). The bonding type of this system is also similar to the one observed for CO_2 clathrate (Figs. 6(e) and 6(f)). The ELF configuration for GeO_2 clathrate is also similar to CO_2 isostructure. It is interesting to note that the ionicity as calculated from Bader analysis increases from CO_2 to SiO_2 and then decreases to GeO_2 . On the other hand, the SiO_2 clathrate is the only substance that presents strongly localized electrons at the oxygen-silicon atom boundary (Figure 6). This

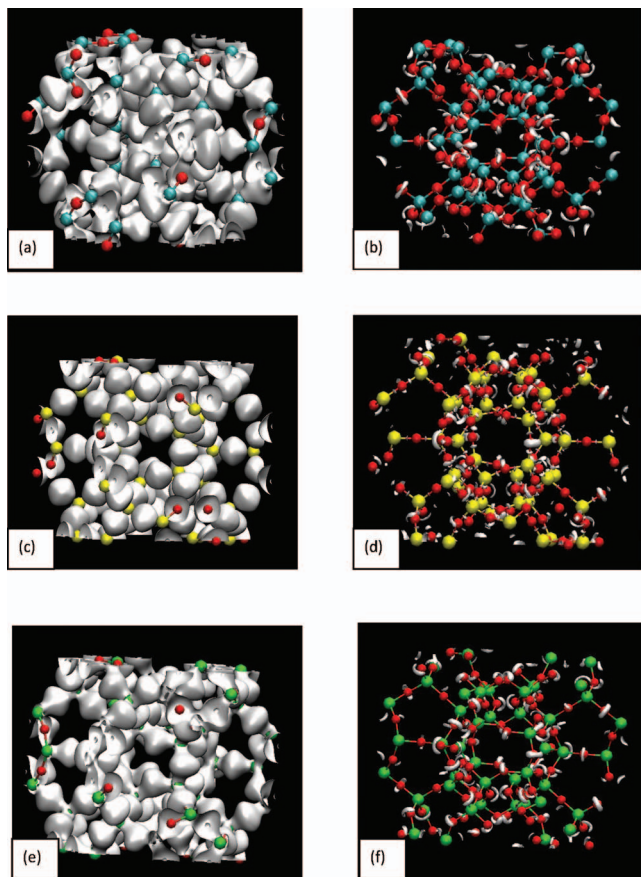


FIG. 6. ELF isosurfaces for CO_2 , SiO_2 and GeO_2 clathrates. Blue, yellow, green, and red spheres represent carbon, silicon, germanium, and oxygen atoms, respectively. The ELF isosurface value of 0.506 (a,c,e) and ELF = 0.894 (b,d,f).

unique electron structural property might stem from the different energies of the C, Si and Ge orbitals and serve as the reason why SiO_2 adopts a diverse phase diagram. The total and projected electronic density of state of elemental oxide clathrates are shown in Fig. 7. The GeO_2 clathrate shows the smallest gap value (2.75 eV) compared with the band gap of CO_2 clathrate (5.10 eV) and SiO_2 clathrate (5.58 eV). The band gap of SiO_2 clathrate is around 5.58 eV. This is similar to that of quartz, around 5-6 eV, as reported in the previous first-principles studies by using local density approximation (LDA).⁵⁰ The band gap of CO_2 clathrate is around 5.1 eV, which is close to that of quartz-type structure of CO_2 phase, around 5 eV, but smaller than that of the β -cristobalite-like CO_2 , around 7 eV. This band gap difference implies that a different band gap as large as 2 eV could be just induced by a slightly different local structure, not necessarily to be linked with vast coordination number changes. From this regard, it is not surprising that the band gap of GeO_2 is around 2.75 eV, whereas the reported GGA band gap of quartz-type GeO_2 is around 5.0 eV.³¹ Finally, it is also interesting to note that the GGA band gap of rutile-type GeO_2 is around 2.4 eV.³¹

It has been suggested that because of the isostructural correlation between CO_2 , GeO_2 and SiO_2 quartz phases, their electronic structure would be similar.^{28,31,50} In order to extend this discussion for the bonding nature in clathrates isostructural phase, let us first, analyze the details of the SiO_2 clathrate

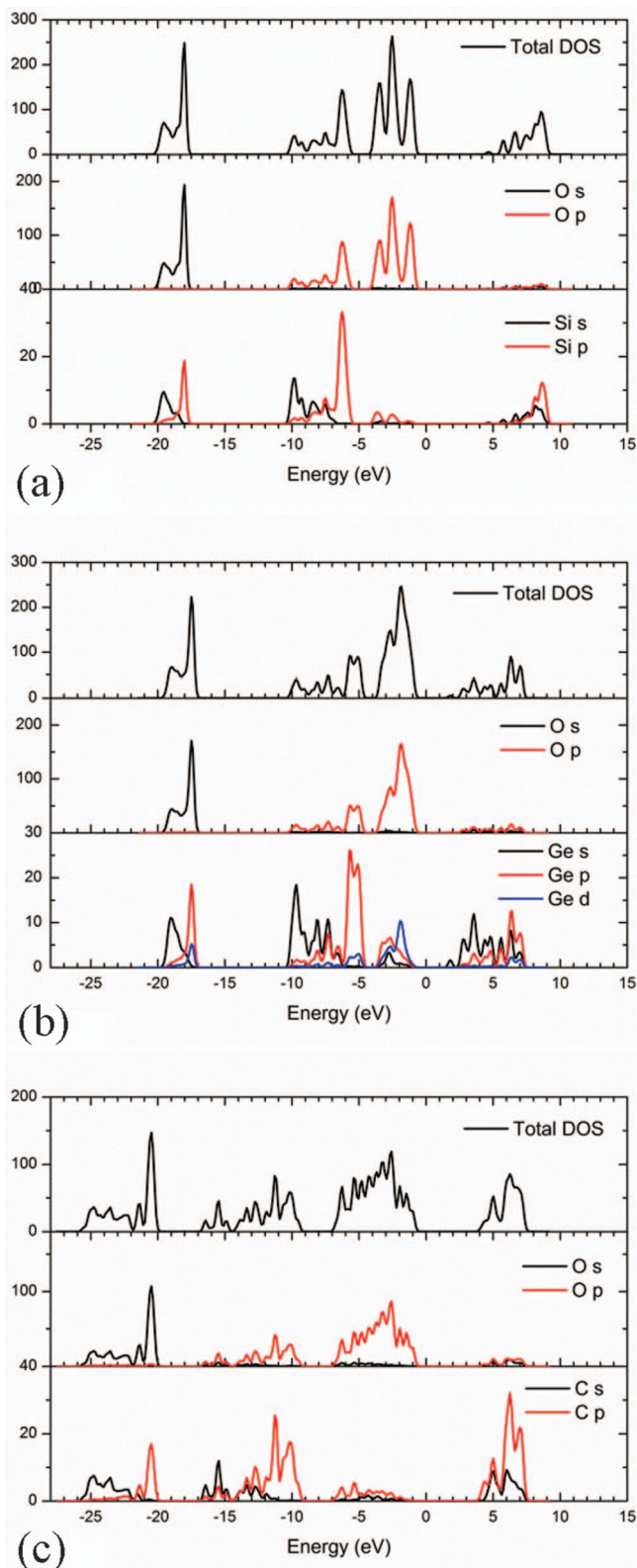


FIG. 7. Comparison of the total and projected electronic density of states of SiO_2 (a), GeO_2 (b), and CO_2 clathrates (c).

electronic structure to guide us in the comparison with the GeO_2 and CO_2 cases. Analysis of the SiO_2 clathrate total and projected density of states (DOS) shows four distinct regions. In region 1 (between -20 and -17 eV), the lower-lying states around -19.5 eV originates from the Si 2s and O 2s orbitals,

while the peak around 18.0 eV the states are composed by 2p orbitals of Si and O p states. For region 2 (between -10 and -5 eV), we can distinguish two main components one below -7 eV that is composed mainly by hybridization of Si 2s and O 2p orbitals, and another above -7 eV, that is originated by the Si 2p and O 2p states. In the valence region (region 3) near the Fermi level, the localized states are basically composed by p states from Si and O. The HOMO was identified to be localized on the 48l and 8e O sites, while the LUMO has mainly an s character orbitals and observed for all O sites (48l, 24k, 12f and 8e).

Compared with other SiO₂ polymorphs and the pressure effect on electronic properties, our calculations suggest a similar trend for the clathrate as observed for SiO₂ quartz. The differences are mainly due to the Si-O-Si angles between the structures, which lead to a separation on the two upper valence bond for the clathrate case, in opposite to quartz at 0 GPa. It is interesting to note that the clathrate behavior is in an opposite direction of the positive pressure effects on quartz phase, where there is a merge in those valence bands. This is consistent with the clathrate open structure. In this way, the clathrate structure could be seen as a negative pressure effect on the electronic structure on four-coordinated SiO₂ phases.

The GeO₂ clathrate projected DOS has similar features compared with the SiO₂ case. In general, the 4 different regions in GeO₂ are narrower than the ones observed in SiO₂. The HOMO in this case, it is localized mainly in the O 24 k sites, while LUMO has been identified in the same crystallographic oxygen sites as the SiO₂ one, but with a s-p character. In addition, every Ge presents LUMO states with s-p character.

Additionally, CO₂ clathrate has the 4 regions broader than the SiO₂ case. Analysis of the CO₂ clathrate total and projected DOS shows four distinct regions. The lower-lying states below -22 eV originates from the C 2s and O 2s orbitals, while between -22 and 20 eV the states are composed by 2p orbitals of C and O. States in the region between -17 and -10 eV, are composed mainly by hybridization of C and O p orbitals around -11 eV and C 2s and O 2p orbitals below -15 eV. The states in the valence band region between -7 and 0 eV near the Fermi level are spread. For CO₂ clathrate, the HOMO states were identified to be related to the O 48l and 24k sites. On the other hand, the states in the conduction band region between 4 and 7 eV has mainly C 2s and 2p contribution. Interestingly, the LUMO states has been identified by the C 6c sites and p-orbitals, in opposite to the observed for the SiO₂ and GeO₂ clathrates, where the LUMO was assigned to the 48l, 24k and 12f O sites. The heterogeneity of electron at different symmetry sites and the inversion of the s-orbitals and p-orbitals of conduction bands of carbon in the CO₂ clathrate may be a sign of the electronic instability of that clathrate at low pressures.

IV. CONCLUSIONS

Although, theoretically possible adding the CO₂ guest-free clathrate into CO₂ 3-dimensional network solid phases, the proposed CO₂ guest-free clathrate phase was found in our

calculations hardly to be synthesized due to the large energy difference with respect to other stable phases. However, for the guest-free clathrate GeO₂, we found that its total energy is lower than that of α -quartz and rutile for slightly negative pressures, which could give us a clue for possible synthesis routes. We also found meta-GGA can fix the problem of GGA calculation to describe the stability of low-pressure SiO₂ polymorphs. In perspective, the mechanical properties bulk modulus CO₂ phase shows highest value than the analogous SiO₂ and GeO₂ phases, as response of the rigidity of the inter tetrahedron angle and shortest bond length. Temperature effect has arisen in SiO₂ clathrate, the softening of materials showed in the decreasing of bulk modulus with elevated temperature. In particular, our work has enriched the diversity of CO₂, SiO₂ and GeO₂ polymorphism terms of their relative thermodynamic stability and mechanical properties.

ACKNOWLEDGMENTS

The authors thank JOGMEC, JST/JICA-SATREPS, and JAPEX for financial support and Sandro Scandolo and Jeverson T. Arantes for valuable comments. C.R.M. acknowledges the Brazilian agencies CNPq, FAPESP and UFABC for funding, and is grateful for JSPS Invitation Fellowship Program for supporting his short visit in Japan. M.L. acknowledges the Japanese Government (Monbukagakusho) for the scholarship.

- ¹V. Iota, C. S. Yoo, and H. Cynn, *Science* **283**, 1510 (1999).
- ²C. S. Yoo, H. Cynn, F. Gygi, G. Galli, V. Iota, M. Nicol, S. Carlson, D. Hausermann, and C. Mailhiot, *Phys. Rev. Lett.* **83**, 5527 (1999).
- ³J. Dong, J. K. Tomfohr, and O. F. Sankey, *Phys. Rev. B* **61**, 5967 (2000).
- ⁴Y. Seto, D. Nishio-Hamane, T. Nagai, N. Sata, and K. Fujino, *J. Phys.: Conf. Series* **215**, 012015 (2010).
- ⁵F. Datchi, B. Mallick, A. Salamat, and S. Ninet, *Phys. Rev. Lett.* **108**, 125701 (2012).
- ⁶M. Santoro, F. A. Gorelli, R. Bini, J. Haines, O. Cambon, C. Levelut, J. A. Montoya, and S. Scandolo, *Proc. Natl. Acad. Sci. U.S.A.* **109**, 5176 (2012).
- ⁷M. Santoro, F. A. Gorelli, R. Bini, G. Ruocco, S. Scandolo, and W. A. Crichton, *Nature (London)* **441**, 857 (2006).
- ⁸G. S. Smith and P. B. Isaacs, *Acta Cryst.* **17**, 842 (1964).
- ⁹E. D. Sloan, *Clathrate Hydrates of Natural Gases*, 2nd ed. (Dekker, New York, 1998).
- ¹⁰R. K. McMullan and G. A. Jeffrey, *J. Chem. Phys.* **42**, 2725 (1965).
- ¹¹J. A. Ripmeester, J. S. Tse, C. I. Ratcliffe, and B. M. Powell, *Nature (London)* **325**, 135 (1987).
- ¹²Y.-T. Seo and H. Lee, *J. Phys. Chem. B* **105**, 10084 (2001).
- ¹³W. L. Mao, H.-K. Mao, A. F. Goncharov, V. V. Struzhkin, Q. Guo, J. Hu, J. Shu, R. J. Hemley, M. Somayazulu, and Y. Zhao, *Science* **297**, 2247 (2002).
- ¹⁴W. Shimada, M. Shiro, H. Kondo, S. Takeya, H. Oyama, T. Ebinuma, and H. Narita, *Acta Cryst. C* **61**, 65 (2005).
- ¹⁵H. Lu, Y.-T. Seo, J.-W. Lee, I. Moudrakovski, J. A. Ripmeester, N. R. Chapman, R. B. Coffin, G. Gardner, and J. Pohlman, *Nature (London)* **445**, 303 (2007).
- ¹⁶B. J. Skinner and D. E. Appleman, *Am. Mineral.* **48**, 854 (1963).
- ¹⁷B. Kamb, *Science* **148**, 232 (1965).
- ¹⁸T. Nakagawa, K. Kihara, and K. Harada, *Am. Mineral.* **86**, 1506 (2001).
- ¹⁹H. W. Xu, J. Z. Zhang, Y. S. Zhao, G. D. Guthrie, D. D. Hickmott, and A. Navrotsky, *Am. Miner.* **92**, 166 (2007).
- ²⁰T. Yagi, E. Iida, H. Hirai, N. Miyajima, T. Kikegawa, and M. Bunno, *Phys. Rev. B* **75**, 174115 (2007).
- ²¹Y. Liang, F. O. Ogundare, C. R. Miranda, J. K. Christie, and S. Scandolo *J. Chem. Phys.* **134**, 074506 (2011).
- ²²C. R. Miranda and A. Antonelli, *Phys. Rev. B* **74**, 153203 (2006).
- ²³A. Simon and K. Peters, *Acta Cryst. B* **36**, 2750 (1980).
- ²⁴K. Aoki, H. Yamawaki, M. Sakashita, Y. Gotoh, and K. Takemura, *Science* **263**, 356 (1994).

- ²⁵S. Serra, C. Cavazzoni, G. L. Chiarotti, S. Scandolo, and E. Tosatti, *Science* **284**, 788 (1999).
- ²⁶S. A. Bonev, F. Gygi, T. Ogitsu, and G. Galli, *Phys. Rev. Lett.* **91**, 065501 (2003).
- ²⁷J. Dong, J. K. Tomfohr, O. F. Sankey, K. Leinenweber, M. Somayazulu, and P. F. McMillan, *Phys. Rev. B* **62**, 14685 (2000).
- ²⁸B. Holm, R. Ahuja, A. Belonoshko, and B. Johansson, *Phys. Rev. Lett.* **85**, 1258 (2000).
- ²⁹J. Sun, D. D. Klug, R. Martonak, J. A. Montoya, M.-S. Lee, S. Scandolo, and E. Tosatti, *PNAS* **106**, 6077 (2009).
- ³⁰M.-S. Lee, J. A. Montoya, and S. Scandolo, *Phys. Rev. B* **79**, 144102 (2009).
- ³¹D. M. Christie and J. R. Chelikowsky, *Phys. Rev. B* **62**, 14703 (2000).
- ³²V. P. Prakapenka, G. Shen, L. S. Dubrovinsky, M. L. Rivers, and S. R. Sutton, *J. Phys. Chem. Solids* **65**, 1537 (2004).
- ³³J. Hafner, *Comp. Phys. Comm.* **177**, 6 (2007).
- ³⁴Y. Wang and J. P. Perdew, *Phys. Rev. B* **45**, 13244 (1992).
- ³⁵D. R. Hamann, *Phys. Rev. Lett.* **76**, 660 (1996).
- ³⁶J. Hafner, *J. Comput. Chem.* **29**, 2044 (2008).
- ³⁷T. Demuth, Y. Jeanvoine, J. Hafner, and J. G. Angyan, *J. Phys.: Condens. Matter* **11**, 3833 (1999).
- ³⁸P. Tangney and S. Scandolo, *J. Chem. Phys.* **117**, 8898 (2002).
- ³⁹D. Herzbach, K. Binder, and M. H. Müser, *J. Chem. Phys.* **123**, 124711 (2005).
- ⁴⁰Y. Liang, C. R. Miranda, and S. Scandolo, *Phys. Rev. B* **75**, 024205 (2007).
- ⁴¹Y. Liang, C. R. Miranda, and S. Scandolo, *Phys. Rev. Lett.* **99**, 215504 (2007).
- ⁴²Y. Liang, C. R. Miranda, and S. Scandolo, *J. Chem. Phys.* **125**, 194524 (2006).
- ⁴³E. R. Cope and M. T. Dove, *J. Phys.: Condens. Matter* **22**, 125401 (2010).
- ⁴⁴D. A. Keen and M. T. Dove, *J. Phys.: Condens. Matter* **11**, 9263 (1999).
- ⁴⁵L. Pauling, *The Nature of the Chemical Bond*, 3rd Ed. (Cornell University Press, Ithaca, 1960).
- ⁴⁶R. F. W. Bader, *Atoms in Molecules: A Quantum Theory. International Series of Monographs on Chemistry* (Clarendon Press, Oxford, 1990).
- ⁴⁷A. D. Becke, and K. E. Edgecombe, *J. Chem. Phys.* **92**, 5397 (1990).
- ⁴⁸B. Silvi and A. Savin, *Nature* **371**, 683 (1994).
- ⁴⁹A. Savin, R. Nesper, S. Wengert, and T. F. Fassler, *Angew. Chem. Int. Ed. Engl.* **36**, 1808 (1997).
- ⁵⁰N. Binggeli, N. Troullier, J. L. Martins, and J. R. Chelikowsky, *Phys. Rev. B* **44**, 4771–4777 (1991).